

# Plasminogen activation independent of uPA and tPA maintains wound healing in gene-deficient mice

Leif R Lund<sup>1,\*</sup>, Kirsty A Green<sup>1</sup>, Allart A Stoop<sup>2</sup>, Michael Ploug<sup>1</sup>, Kasper Almholt<sup>1</sup>, Jennifer Lilla<sup>3</sup>, Boye S Nielsen<sup>1</sup>, Ib J Christensen<sup>1,4</sup>, Charles S Craik<sup>2</sup>, Zena Werb<sup>3</sup>, Keld Danø<sup>1</sup> and John Rømer<sup>1</sup>

<sup>1</sup>Finsen Laboratory, Rigshospitalet, Strandboulevarden 49, Copenhagen, Denmark, <sup>2</sup>Department of Pharmaceutical Chemistry, University of California, San Francisco, CA, USA and <sup>3</sup>Department of Anatomy, University of California, San Francisco, CA, USA

**Simultaneous ablation of the two known activators of plasminogen (Plg), urokinase-type (uPA) and the tissue-type (tPA), results in a substantial delay in skin wound healing. However, wound closure and epidermal re-epithelialization are significantly less impaired in uPA;tPA double-deficient mice than in Plg-deficient mice. Skin wounds in uPA;tPA-deficient mice treated with the broad-spectrum matrix metalloproteinase (MMP) inhibitor galardin (N-[(2R)-2-(hydroxamido-carbonylmethyl)-4-methylpentanoyl]-L-tryptophan methylamide) eventually heal, whereas skin wounds in galardin-treated Plg-deficient mice do not heal. Furthermore, plasmin is biochemically detectable in wound extracts from uPA;tPA double-deficient mice. *In vivo* administration of a plasma kallikrein (pKal)-selective form of the serine protease inhibitor ecotin exacerbates the healing impairment of uPA;tPA double-deficient wounds to a degree indistinguishable from that observed in Plg-deficient mice, and completely blocks the activity of pKal, but not uPA and tPA in wound extracts. These findings demonstrate that an additional plasminogen activator provides sufficient plasmin activity to sustain the healing process albeit at decreased speed in the absence of uPA, tPA and galardin-sensitive MMPs and suggest that pKal plays a role in plasmin generation.**

*The EMBO Journal* (2006) 25, 2686–2697. doi:10.1038/sj.emboj.7601173; Published online 8 June 2006

**Subject Categories:** molecular biology of disease

**Keywords:** fibrinolysis; plasma kallikrein; plasmin; uPA-, tPA- and plasminogen-deficient mice; wound healing

## Introduction

Confined proteolytic degradation of the extracellular matrix by the concerted action of the serine protease plasmin and

members of the matrix metalloprotease (MMP) family is considered to play a key role in a variety of physiological and pathological processes involving tissue remodeling and cell migration, including cancer invasion (Danø *et al*, 2005; Egeblad and Werb, 2002). A role for the plasmin precursor plasminogen (Plg) in tissue remodeling processes has been conclusively demonstrated by studies of skin wound healing (Rømer *et al*, 1996), cancer metastasis (Bugge *et al*, 1998), post-lactational mammary gland involution (Lund *et al*, 2000) and placental development (Solberg *et al*, 2003) in mice with a disrupted Plg gene. Plasmin is formed from Plg by cleavage catalyzed by Plg activators. Two physiologically active mammalian Plg activators are known, the urokinase-type (uPA) and the tissue-type (tPA) (Danø *et al*, 1985; Collen and Lijnen, 2005). uPA is secreted as an inactive precursor, pro-uPA, which can bind to the uPA receptor (uPAR), a glycolipid-anchored membrane protein with three-fold finger domains (Llinas *et al*, 2005). Pro-uPA is activated to uPA by plasmin while bound to uPAR, and receptor-bound uPA can activate Plg (Ploug, 2003). Concomitant binding of pro-uPA and Plg to cell surfaces strongly accelerates plasmin generation owing to an increased efficiency of the reciprocal activation of the two proenzymes (Ellis *et al*, 1991). tPA-directed plasminogen activation is accelerated by concomitant binding of tPA and Plg to fibrin (Carmeliet *et al*, 1994; Collen and Lijnen, 2005). Preferential sites for the uPA and tPA pathways of Plg activation are therefore surfaces of uPAR-expressing cells and fibrin deposits, respectively. In accordance, the primary established functions of uPA are within tissue remodeling processes (Danø *et al*, 1999), whereas those of tPA are within vascular thrombolysis (Collen and Lijnen, 2005). Despite this divergence in their basic biological functions, uPA and tPA can to some extent serve as mutual, functional substitutes, as has been observed in gene-deficient mice (Carmeliet *et al*, 1994; Bugge *et al*, 1996a). In addition to uPA and tPA, a few other serine proteases such as the blood coagulation factors XI and XII and plasma kallikrein are capable of activating plasminogen in test tubes (Danø *et al*, 1985). However, the physiological impact of such activators has not been thoroughly demonstrated *in vivo* during, for example, skin wound healing. In mammary gland involution, it was suggested that plasma kallikrein (pKal) is a Plg activator during adipocyte differentiation (Selvarajan *et al*, 2001).

During healing of skin wounds, the migrating leading-edge keratinocytes express uPA and uPAR. tPA is more scarcely expressed but has been detected in a few keratinocytes late in the re-epithelialization of human wounds (Rømer, 2003). In Plg-deficient mice there is a pronounced delay in wound healing characterized by a decreased rate of migration of keratinocytes from the wound edges and an accumulation of fibrin in front of the leading-edge keratinocytes, suggesting that the delay is owing to a diminished ability of these cells to proteolytically dissect their way through the extracellular

\*Corresponding author. Finsen Laboratory, Copenhagen University Hospital, Strandboulevarden 49, 2100 Copenhagen, Denmark.

Tel.: 45 35455907; Fax: 45 35385450; E-mail: lund@inet.uni2.dk

<sup>4</sup>Present address: Department of Surgical Gastroenterology, Hvidovre Hospital, DK-2650 Hvidovre, Denmark

Received: 13 September 2005; accepted: 8 May 2006; published online: 8 June 2006

matrix (Rømer *et al*, 1996). This interpretation is supported by the observation that skin wound healing is restored in mice deficient in both *plasminogen* and *fibrin* (Bugge *et al*, 1996b). Although delayed, complete wound healing is eventually achieved in all *Plg*-deficient mice. Several MMPs, including MMP3, MMP9 and MMP13, are expressed in murine leading-edge keratinocytes (Madlener *et al*, 1998; Lund *et al*, 1999), and wound healing is severely impaired in transgenic mice with human collagenase-1-resistant collagen I (Beare *et al*, 2003). Treatment of wild-type mice with a broad-spectrum MMP inhibitor, galardin (N-[(2R)-2-(hydroxamido-carbonylmethyl)-4-methylpentanoyl]-L-tryptophan methylamide), causes a delay in wound healing time, but all wounds do eventually heal. However, when *Plg*-deficient mice are treated with galardin, healing is completely arrested, demonstrating that protease activity is essential for wound healing and that there is a functional overlap between the two classes of matrix-degrading proteases in this process (Lund *et al*, 1999).

In order to study the relative contribution of the individual plasminogen activators during wound healing, we have examined the impact on skin repair of single deficiencies in *uPA*, *tPA* and *Plg* as well as double deficiency in *uPA* and *tPA*. We now provide *in vivo* biochemical and genetic evidence to demonstrate first a functional overlap between *uPA* and *tPA*, and second the existence of at least one additional *Plg* activator contributing to wound healing. Further experimental evidence points to plasma kallikrein as the possible third plasminogen activator with *in vivo* activity during skin wound healing.

## Results

### Functional overlap between *uPA* and *tPA* in wound healing

We first examined the effect on wound healing of single deficiencies in *uPA* and *tPA* and double deficiency in both activators. Standardized 20 mm long, full thickness, incisional wounds were generated in wild-type mice ( $n = 30$ ),

*uPA*-deficient mice ( $n = 13$ ), *tPA*-deficient mice ( $n = 17$ ) and mice double-deficient for *uPA* and *tPA* ( $n = 13$ ). All mice were F2-generation siblings derived from backcrossing single-deficient mice into the C57Bl/6J strain for 16 generations. The wounds were examined grossly by visual inspection, and the wound lengths measured three times a week. Immediately after surgery, the wounds were spindle-shaped with well-separated incision edges and the underlying muscle fascia was exposed. By the second day post-wounding, the wounds were covered by a dehydrated wound crust, which was gradually lost as healing progressed. Lesions were scored as fully healed when there was a complete loss of the wound crust and closure of the incision interface with restoration of the epidermal covering. Immediately after the wounds were scored as healed by gross inspection, the wounded skin was removed for histological examination. Healing was in all cases verified by the presence of an intact multilayered epidermis (see Figure 3).

The mean times to complete healing for mice with single deficiencies in either *uPA* or *tPA* was  $18.2 \pm 2.7$  and  $17.6 \pm 2.8$  days, respectively, which were similar to the healing time of  $16.9 \pm 3.2$  days in wild-type mice (Table I; Figure 1A). In mice double-deficient for *uPA* and *tPA*, the mean healing time increased to  $31.2 \pm 11.3$  days, a significant delay in skin wound healing compared to the wild-type mice ( $P = 0.0006$ ) and also to the *uPA* ( $P = 0.0008$ ) or *tPA* ( $P = 0.0007$ ) single-deficient mice (Table I; Figure 1A). The combined ablation of *uPA* and *tPA* thus results in a pronounced impairment of wound healing, whereas there is virtually no effect on wound healing of deficiency in either of the two genes alone. We conclude that the presence of either *uPA* or *tPA* is required to maintain full wound healing capacity and that there is a functional overlap between the two.

### Skin wound healing is less impaired in mice double deficient for *uPA* and *tPA* compared to *Plg*-deficient mice

We next compared the efficiency of the skin wound healing in the *uPA,tPA* double-deficient mice with that in *Plg*-deficient

**Table I** Effect of *uPA*, *tPA* and *Plg* single deficiencies, *uPA,tPA* double-deficiency and galardin treatment on wound healing time

Group	Genotype	Number of backcrossings	Treatment	Number of mice	Mean healing time (days)	s.d.	P-value
1	Wild-type	16	None	30	16.9	3.2	
2	<i>uPA</i> -/-; <i>tPA</i> +/+	16	None	13	18.2	2.7	2 versus 1 NS <sup>a</sup>
3	<i>uPA</i> +/+; <i>tPA</i> -/-	16	None	17	17.6	2.8	3 versus 1 NS <sup>a</sup>
4	<i>uPA</i> -/-; <i>tPA</i> -/-	16	None	13	31.2	11.3	4 versus 1 0.0006
5	Wild-type	21	None	24	16.8	2.2	
6	<i>Plg</i> -/-	21	None	20	42.9	15.6	6 versus 5 0.0001; 6 versus 4 0.03
7	Wild-type	16	Mock	16	17.0	3.7	
8	Wild-type	16	Galardin <sup>b</sup>	10	22.3	5.5	8 versus 7 0.008
9	<i>uPA</i> -/-; <i>tPA</i> -/-	16	Mock	13	30.2	10.0	9 versus 7 0.0004
10	<i>uPA</i> -/-; <i>tPA</i> -/-	16	Galardin <sup>b</sup>	7	45.9	6.9	10 versus 9 0.002
11	Wild-type	21	Mock	15	19.0	2.9	
12	Wild-type	21	Galardin <sup>b</sup>	15	24.9	3.8	12 versus 11 0.0001
13	<i>Plg</i> -/-	21	Mock	14	50.9	19.3	13 versus 11 0.0001; 13 versus 9 0.002
14	<i>Plg</i> -/-	21	Galardin <sup>b</sup>	12	> 70 days <sup>c</sup>		14 versus 13 0.0001; 14 versus 10 0.0001

<sup>a</sup>Not significant ( $P > 0.05$ ).

<sup>b</sup>100 mg/kg daily.

<sup>c</sup>No wounds healed at end of galardin treatment.

Abbreviations: *Plg*, plasminogen; *tPA*, tissue-type plasminogen activator; *uPA*, urokinase-type plasminogen activator.

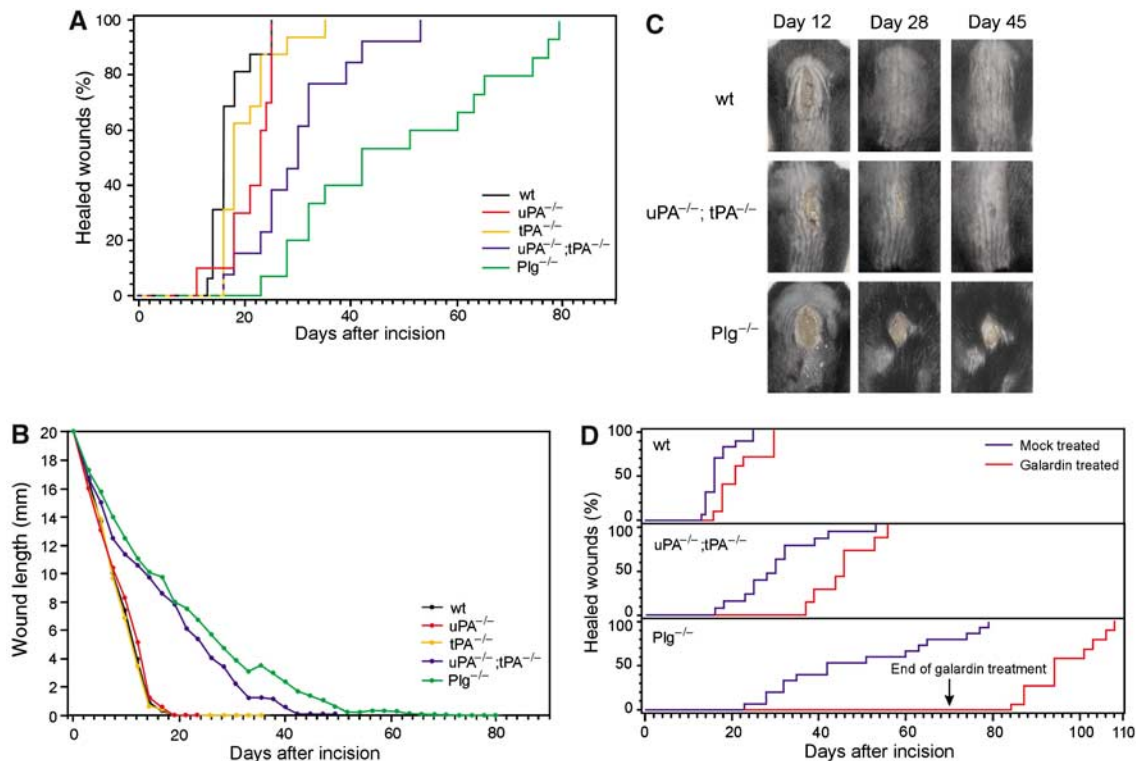


**Figure 1** Time course for healing of full-thickness skin wounds in wild-type, *tPA*-deficient, *uPA*-deficient, *uPA;tPA* double-deficient and *Plg*-deficient mice. **(A)** The percentage fraction of mice with complete gross healing is plotted versus time after the incision. A modest and nonsignificant delay was observed in *tPA* single-deficient and *uPA* single-deficient mice compared to wild-type mice, whereas a significant delay was observed in *uPA;tPA* double-deficient mice. In *Plg*-deficient mice, there was an even more pronounced delay and the healing occurred significantly later than in the *uPA;tPA* double-deficient mice. **(B)** The average wound length is plotted versus time after incision. The average wound length of wild-type, *uPA*-deficient and *tPA*-deficient mice was indistinguishable until re-epithelialization. In contrast, the wound length of *uPA;tPA* double-deficient mice was significantly increased compared to either wild-type or *uPA*- or *tPA* single-deficient mice. The average wound length of *Plg*-deficient mice was significantly increased compared to *uPA;tPA* double-deficient mice. **(C)** Examples of the progress of wound repair in wild-type, *uPA;tPA* double-deficient and *Plg*-deficient mice. **(D)** Galardin or mock treatment of wild-type, *uPA;tPA* double-deficient and *Plg*-deficient mice. The percentage fraction of wounds healed is plotted versus time after the incision. The wild-type and *uPA;tPA* double-deficient mice treated with galardin exhibited a delay in healing compared to mock-treated mice but all wounds eventually healed. In contrast, galardin treatment of *Plg*-deficient mice completely blocked healing. However, this arrest was reversible as cessation of galardin treatment in these mice at day 70 resulted in completion of healing, so that the wounds were completely healed within 28 days.

mice. For this purpose, we used *Plg* gene-targeted mice backcrossed into the C57Bl/6J strain for 21 generations. These heterozygous *Plg* gene-deficient mice were interbred, resulting in an F1 generation of mice, of which the homozygous *Plg*-deficient mice ( $n=20$ ) and their wild-type siblings ( $n=24$ ) were used in the experiment.

The mean wound healing time in the *Plg*-deficient mice was  $42.9 \pm 15.6$  days, whereas the mean healing time in the control group of wild-type mice was  $16.8 \pm 2.2$  days (Table I; Figure 1A) in accordance with previous studies (Rømer *et al*, 1996). The mean healing time in the *Plg*-deficient mice was also significantly longer ( $P=0.03$ ) than the  $31.2 \pm 11.3$  days observed in the *uPA;tPA* double-deficient mice as shown in Figure 1A. Importantly, the healing time in the two control groups of wild-type siblings corresponding to the *uPA;tPA* double-deficient and the *Plg*-deficient mice, respectively, were indistinguishable ( $16.9 \pm 3.2$  and  $16.8 \pm 2.2$  days). In a separate experimental setup, wild-type mice obtained by breeding of *MMP-9;Plg* and *MMP3;Plg* double-heterozygous mice exhibited similar healing times ( $17.0 \pm 3.2$  and  $17.8 \pm 3.6$  days). Notably, these were indistinguishable from the healing times in the background strain C57Bl/6J ( $16.3 \pm 2.8$  days). This emphasizes that the observed difference between the *uPA;tPA*

double-deficient and *Plg*-deficient mice is not caused by random genetic differences between the various lines of gene-targeted mice, but is clearly ascribed to a role of *Plg* in wound healing that is not entirely dependent on the presence of the cognate activators *uPA* and *tPA*.

Following wounding, the average wound lengths of wild-type, *uPA* single-deficient and *tPA* single-deficient mice were indistinguishable until completion of re-epithelialization (Figure 1B). As opposed to this, the average wound length in *uPA;tPA* double-deficient mice was significantly increased compared to either wild-type or *uPA*- or *tPA* single-deficient mice ( $P<0.001$ ). Furthermore, the average wound length of *Plg*-deficient mice was significantly increased compared to *uPA;tPA* double-deficient mice ( $P<0.02$ ) (Figure 1B).

#### ***In the presence of galardin, wound healing is delayed in uPA and tPA double-deficient mice but arrested in Plg-deficient mice***

We have previously demonstrated that the MMP inhibitor galardin delays wound healing in wild-type mice and that healing in *Plg*-deficient mice is completely blocked by galardin treatment (Lund *et al*, 1999). We now compared the effect of galardin on skin wound healing in *uPA;tPA*

double-deficient mice and *Plg*-deficient mice. For each of the genotypes, we used mock-treated wild-type mice that were siblings to the gene-deficient mice as controls. By daily administration of galardin at a dose of 100 mg/kg, healing was further delayed in the *uPA;tPA* double-deficient mice (from  $30.2 \pm 10.0$  days in mock-treated mice to  $45.9 \pm 6.9$  days in galardin-treated mice). However, all the galardin-treated *uPA;tPA* double-deficient mice did eventually heal. In contrast, there was a complete arrest of the healing in the galardin-treated *Plg*-deficient mice for the treatment period of 70 days (Table I and Figure 1D). Notably, there was no difference in the wound healing times between the two mock-treated wild-type control groups or between the two galardin-treated wild-type controls (Table I). These findings indicate that the higher wound healing capability in *uPA;tPA* double-deficient mice in comparison with *Plg*-deficient mice is not dependent on a galardin-sensitive protease.

Interestingly, the *Plg*-deficient mice that had been treated with galardin for 70 days were still capable of healing following discontinuation of galardin treatment, and the tissue repair processes were completed within 28 days (see Figure 1D), indicating that the effect of galardin is due to a transient inhibition, and not to permanent defects in the wound-healing program independent of direct protease inhibition.

**Pronounced histological differences between skin wounds in *uPA;tPA* double-deficient and *Plg*-deficient mice**

We next analyzed histological sections of wound sites from mice of the various genotypes at day 10 after incision (Figure 2), at the time point when the wounds were grossly scored as healed, and 1 month after healing (Figure 3). Wounds in wild-type mice obtained from the breeding of both heterozygous *Plg*<sup>+/-</sup> mice and heterozygous *uPA*<sup>+/-</sup>; *tPA*<sup>+/-</sup> mice were indistinguishable with respect to gross healing as well as histology at all time points post-wounding (data not shown).

At 10 days after wounding, the newly formed epidermal layer underneath the wound crust had completely covered the wound gap in the majority of wild-type and *tPA*-deficient mice (Figure 2A; panels a–d). The wound crust was still retained, which explains why these wounds were not yet scored as healed by gross inspection. The epidermal layer had not covered the wound field in most of the *uPA*-deficient mice, but complete epidermal closure was occasionally observed at this time point (Figure 2A; panels e and f). In contrast, none of the wounds in *uPA;tPA* double-deficient or *Plg*-deficient mice were covered by a new epidermal layer at day 10 post-wounding. (Figure 2A; panels g–j). The provisional matrix was almost completely degraded and replaced by newly formed granulation tissue in wild-type and *tPA*-deficient mice at day 10 (Figure 2A; panels a–d). The formation of granulation tissue was less pronounced in the *uPA*-deficient mice and almost completely absent in the area beneath the epidermal outgrowths in the *uPA;tPA* double-deficient and *Plg*-deficient mice (Figure 2A; panels h and j). All *Plg*-deficient mice and most of the mice single deficient in *uPA* or double deficient in *uPA* and *tPA* showed keratinocyte outgrowths that were markedly blunt-ended (Figure 2A; panels f, h and j). In the *Plg*-deficient mice, the keratinocyte outgrowth was covered by a dense layer of

provisional matrix (Figure 2A; panels i and j), with an accumulation of fibrin(ogen) in front of the keratinocytes that was not seen to the same extent in the other genotypes, although considerable amounts of fibrin(ogen) accumulates beneath the epidermal outgrowth in *uPA;tPA* double-deficient mice (Figure 2B; panels a–c).

At the time of gross healing, which occurred from 12 to 80 days after incision depending on the genotype of the mice, the newly formed epidermal layer covering the wound was thickened and multilayered both in wild-type mice and in the various protease-deficient mice (Figure 3A, C and E and data not shown). However, at the time of healing, the overall morphology of the provisional matrix and granulation tissue in the dermis differed between the genotypes. In wild-type, *uPA* single-deficient and *tPA* single-deficient mice, the entire provisional matrix was replaced by a well-organized granulation tissue (Figure 3A and B and data not shown). In contrast, in both *uPA;tPA* double-deficient and *Plg*-deficient mice, large areas of nondegraded provisional matrix were interspersed with foci of apparently normal vessel- and collagen-rich granulation tissue (Figure 3C and E).

At 1 month after completion of re-epithelialization, the area with regenerated tissue could not be distinguished from the adjacent noninjured epidermis in wild-type, *uPA*-deficient, *tPA*-deficient and *uPA;tPA* double-deficient mice (Figure 3B and D, and data not shown), whereas *Plg*-deficient mice still revealed clusters of nondegraded provisional matrix interspersed in areas of granulation tissue (Figure 3F).

**Attenuated defect in keratinocyte re-epithelialization in *uPA;tPA* double-deficient versus *Plg*-deficient mice**

To assess the impact of *uPA*-deficiency, *tPA*-deficiency, *uPA;tPA* double deficiency and *Plg*-deficiency on re-epithelialization by morphometric analysis, we calculated the percentage fraction of the wound width covered by keratinocytes from both sides of the wound. At 10 days after wounding, the re-epithelialization was lower in the mice with single deficiency for *uPA* ( $55 \pm 7\%$ ), double-deficiency for *uPA* and *tPA* ( $53 \pm 4\%$ ) and deficiency for *Plg* ( $45 \pm 7\%$ ), than in both wild-type mice ( $88 \pm 4\%$ ) and *tPA*-deficient mice ( $92 \pm 5\%$ ) (Figure 4A). At day 21 after incision, the fraction of the wound width covered by keratinocytes was significantly lower in *Plg*-deficient mice ( $76 \pm 8\%$ ) than in *uPA;tPA*-deficient mice ( $93 \pm 4\%$ ; *t*-test  $P = 0.001$ ) (Figure 4B). In all other genotypes, the wounds were completely re-epithelialized at this time point.

**Wound extracts contain a fibrinolytic activity corresponding to pKal**

Because previous studies have suggested a role for plasma kallikrein (pKal) in plasminogen activation during adipocyte differentiation (Selvarajan *et al*, 2001), we next analyzed purified pKal and wound extracts for fibrinolytic activities by fibrin/Plg overlay zymography. As shown in Figure 5A, there was a concentration-dependent degradation of fibrin by purified human pKal. The fibrinolytic activity of 0.5 μg pKal is comparable to that of 0.5 ng of purified murine *uPA*. pKal showed lower fibrinolytic activity in the absence of Plg, which indicates that pKal has some Plg-activator activity (Figure 5A).

In wound extracts from wild-type mice, fibrinolytic activities with electrophoretic mobilities corresponding to purified

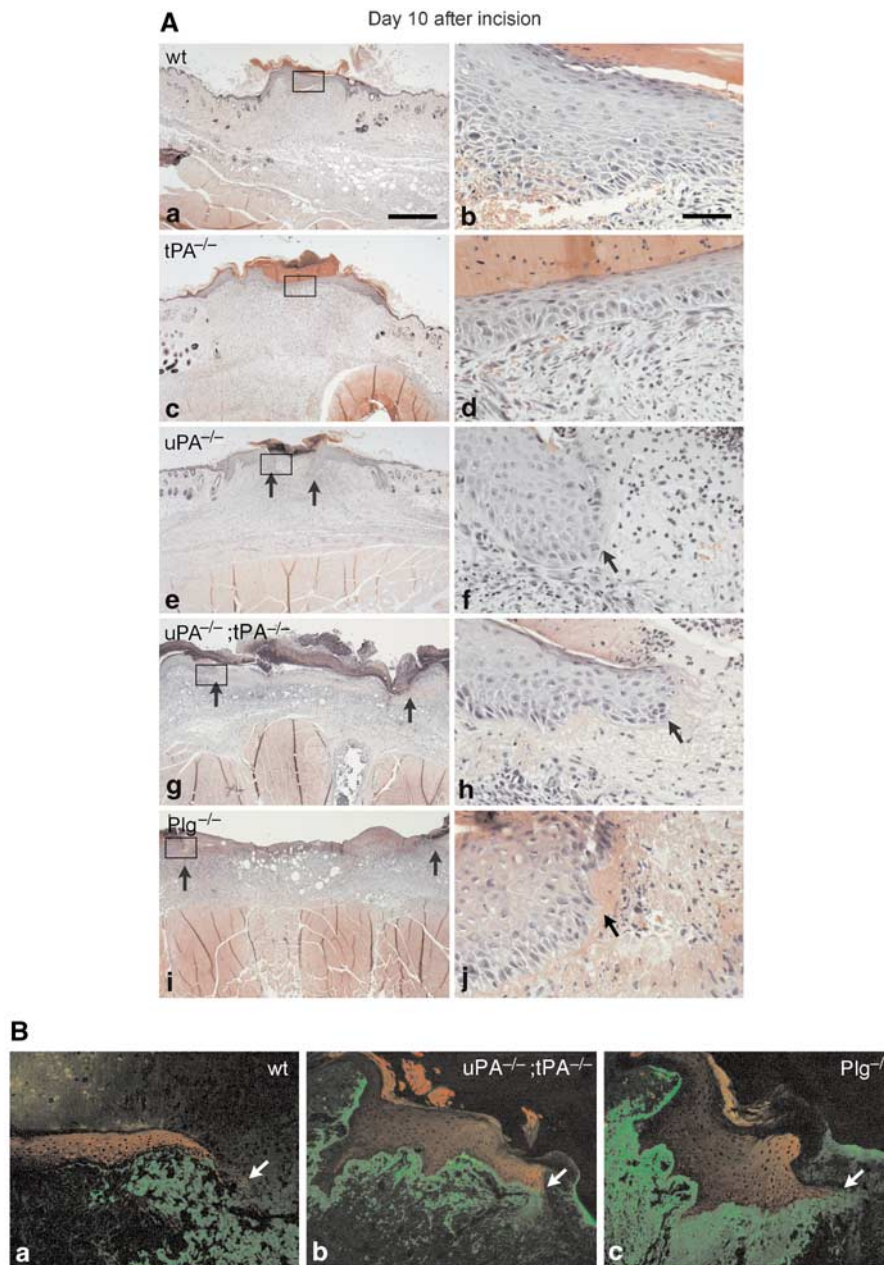


**Figure 2** Analysis of skin wounds in wild-type, *tPA*-deficient, *uPA*-deficient, *uPA;tPA* double-deficient and *Plg*-deficient mice at day 10 after incision. **(A)** H&E-stained sections of wounds from wild-type (a, b), *tPA*-deficient (c, d), *uPA*-deficient (e, f), *uPA;tPA* double-deficient (g, h) and *Plg*-deficient mice (i, j). The boxes in a, c, e, g and i are shown in higher magnification in b, d, f, h, and j. Sections of wild-type (a, b) and *tPA*-deficient mouse wounds (c, d) show a complete multilayered epidermal barrier underneath the wound crust and a newly formed granulation tissue with a small isolated islets of provisional matrix remaining. A section from a *uPA*-deficient mouse (e, f) reveals the leading-edge keratinocytes underneath the wound crust (f). A section of a *uPA;tPA* double-deficient mouse (g, h) reveals migrating keratinocytes surrounded by provisional matrix. Accumulation of amorphous material is observed both in front of, and underneath, the keratinocytes. Similar, but more pronounced accumulations are seen in the sections from *Plg*-deficient mice (i and j). The straight black arrows in (e, g, i, f, h and j) point to the tip of the leading-edge keratinocytes. **(B)** Tissue sections of day 7 wounds from wild-type (a) *uPA;tPA* double-deficient (b) and *Plg*-deficient (c) mice were stained by double immunofluorescence for cytokeratin 8 (red) and fibrin(ogen) (green). Accumulation of immunoreactivity for fibrinogen was observed underneath the keratinocytes in wild-type (a) and *uPA;tPA* double-deficient mice (b). In *Plg*-deficient mice, similar but more pronounced accumulations are seen underneath as well as in front of the keratinocytes (c). The straight white arrows point to the tip of the leading-edge keratinocytes. Bar: Aa, c, e, g and i ~140  $\mu$ m; Ab, d, f, h and j ~35  $\mu$ m.

*uPA* and *pKal* were detected after prolonged development of the fibrin/*Plg* zymograms (Figure 5B). After standard development of the zymograms, *uPA* activity was found in extracts from *tPA*-deficient and *Plg*-deficient mice, whereas virtually no *uPA* was visible in the wild-type wounds, suggesting an upregulation of *uPA* in *tPA*- and *Plg*-deficient wounds

(Figure 6A). The extracts of all genotypes contained a substantial amount of fibrinolytic activity with an electrophoretic mobility corresponding to purified *pKal* (Figures 5B and 6A). No other fibrinolytic activity was observed. In zymograms without *Plg*, all fibrin-degrading activities in the extracts were absent (data not shown).

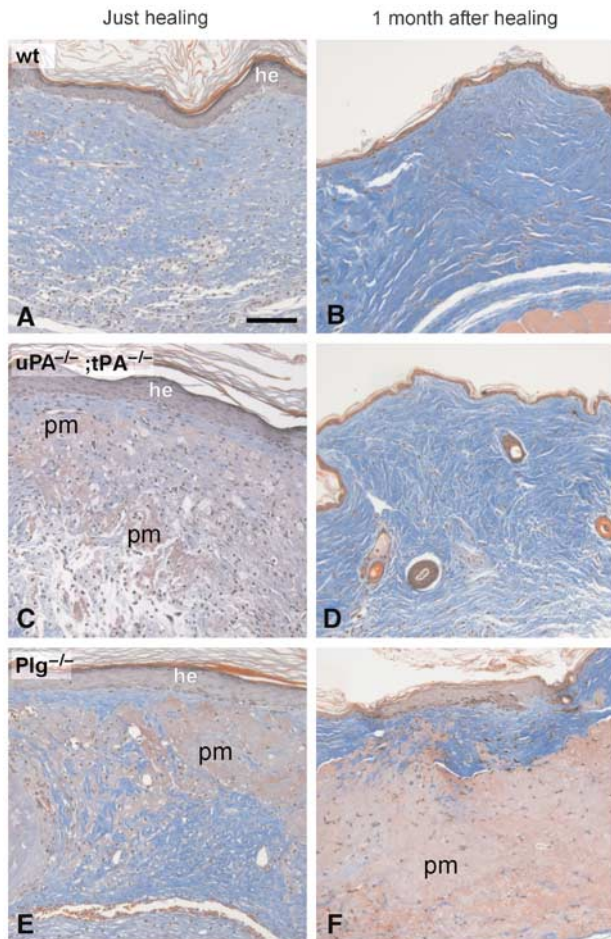


**Figure 3** Analysis of skin wounds in wild-type, *uPA;tPA* double-deficient and *Plg*-deficient mice at the time of healing and 1 month post-healing Trichrome-stained sections of wounds from wild-type (A, B), *uPA;tPA* double-deficient (C, D) and *Plg*-deficient mice (E, F). Sections of tissue isolated just after healing reveal an intact, but hyperplastic epidermis (he), in wild-type mice (A), the provisional matrix has been completely replaced by granulation tissue, whereas in *uPA;tPA* double-deficient and *Plg*-deficient mice, larger areas of nondegraded provisional matrix (pm) were interspersed in the granulation tissue (C, E). At 1 month after healing, wild-type (B) and *uPA;tPA* double-deficient (D) mice all reveal a normal-looking epidermis and dermis, whereas in the *Plg*-deficient mice the epidermis is hyperplastic and the dermis is abnormal with abundant accumulations of undegraded provisional matrix (F). Bar: 60  $\mu$ m.

We used a modified form of the bacterial serine protease inhibitor ecotin<sup>7-29</sup> that is highly selective for pKal and has no inhibitory effect towards, for example, plasmin, uPA, tPA or six other closely related serine proteases, for all of which the  $K_i$  is 4–7 orders of magnitude higher (Stoop and Craik, 2003). The activity corresponding to pKal in wound lysates was completely inhibited by ecotin<sup>7-29</sup>, whereas the inhibitor did not block the activity ascribed to either uPA or the corresponding plasmin activity generated by uPA (Figure 6A). To demonstrate directly that pKal can activate Plg, we next analyzed Plg conversion *in vitro* by Western blot analysis. Both uPA and pKal convert Plg to two-chain plasmin, whereas only trace amounts of Plg are cleaved by prekallikrein. The Plg activation by pKal was not caused by trace impurities in the enzyme preparation as it was inhibited by the pKal-specific ecotin<sup>7-29</sup> (Figure 5C).

### Detection of plasmin in wound extracts from *uPA;tPA* double-deficient mice

Western blot analysis reveals comparable levels of Plg in the crude extracts from wild-type, *uPA* single-deficient, *tPA* single-deficient and *uPA;tPA* double-deficient mice. As expected, no Plg was detected in *Plg*-deficient mice (Figure 5D, lanes 3–7). Similar amounts of plasmin A- and B-chains were found in wound extracts prepared from wild-type mice and *tPA*-deficient mice, whereas only low levels of plasmin chains were observed in the crude extract of *uPA*-deficient mice. However, in *uPA;tPA* double-deficient mice, no plasminogen conversion was directly detectable in the crude extracts (Figure 5D, lanes 3–7). To improve sensitivity, we subsequently performed a one-step enrichment of Plg/plasmin in wound extracts by lysine-Sepharose affinity chromatography. This provided the required sensitivity that enabled the detection of trace amounts of the individual plasmin chains present in some of the genotypes. As evident in Figure 5D, lanes 12 and 16, both A- and B-chains of plasmin were indeed detectable in extracts from *uPA;tPA* double-deficient mice demonstrating that Plg can be converted *in vivo* independently of uPA and tPA. Importantly, neither A- nor B-chains were detectable when extract from noninjured skin or plasma from wild-type mice were tested (Figure 5D, lanes 8, 14 and 15), emphasizing that Plg is activated *in vivo* during active tissue remodeling, and that no conversion occurs during the extraction or purification procedures.

### The serine protease inhibitor ecotin<sup>7-29</sup> exacerbates the healing impairment in *uPA;tPA* double-deficient mice

To examine whether pKal has a physiological role during wound healing, we next treated wounded *uPA;tPA*-deficient or *Plg*-deficient mice systemically for 30 days with either vehicle (PBS) or ecotin<sup>7-29</sup>. Ecotin<sup>7-29</sup> treatment of the *Plg*-deficient mice had no effect on the average wound length (Figure 6C). In contrast, ecotin<sup>7-29</sup> treatment of *uPA;tPA* double-deficient mice significantly delayed wound healing compared to vehicle control, as measured by the average wound length at the end of treatment 30 days post-wounding ( $P < 0.03$ ) (Figure 6C). In fact, the wound lengths of ecotin<sup>7-29</sup>-treated *uPA;tPA* double-deficient mice, mock-treated *Plg*-deficient mice and ecotin<sup>7-29</sup>-treated *Plg*-deficient mice were indistinguishable, which indicates that ecotin<sup>7-29</sup> blocks virtually all remaining plasminogen activation in the *uPA;tPA* double-deficient mice. At the end of ecotin<sup>7-29</sup> treatment at day 30 none of the *uPA;tPA* double-deficient wounds (0%) were healed as opposed to 3 out of 8 healed wounds (38%) in the PBS-treated *uPA;tPA* double-deficient mice (Figure 6B). Immediately after discontinuation of the treatment, a rapid completion of healing was observed in the ecotin<sup>7-29</sup>-treated *uPA;tPA* double-deficient mice.

## Discussion

Skin wound healing is impaired in *Plg*-deficient mice (Rømer *et al*, 1996). Through a direct comparison of *Plg* deficiency versus *uPA;tPA* double deficiency, we now show that the healing in mice that lack both *uPA* and *tPA* is significantly less impaired as compared to *Plg*-deficient mice. This difference is based on observations of attenuated impairments in gross healing times as well as re-epithelialization in the *uPA;tPA* double-deficient mice. We have found that gross skin wound

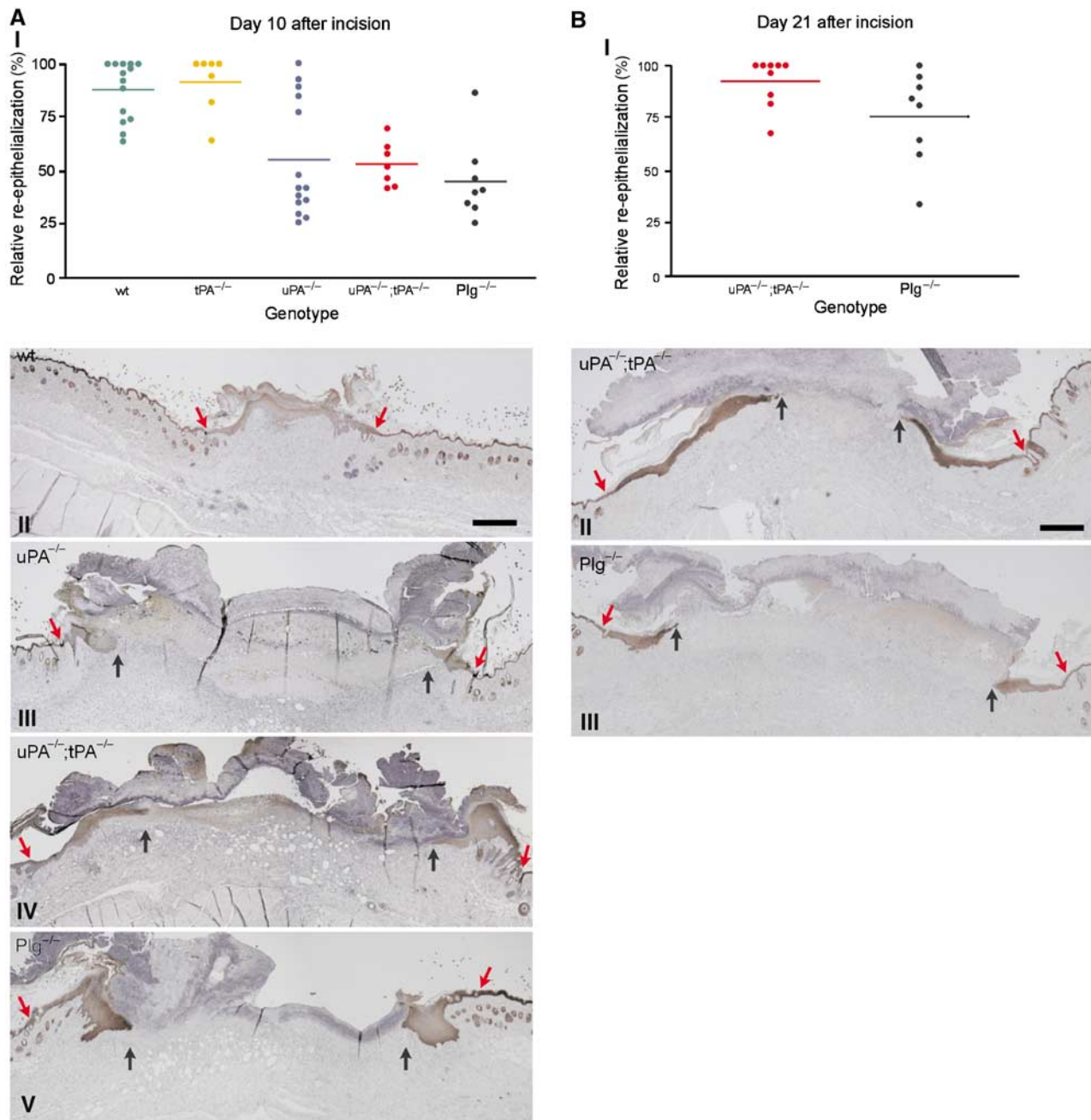


**Figure 4** Morphometric analysis of wound re-epithelialization in wild-type, *tPA*-deficient, *uPA*-deficient, *uPA;tPA* double-deficient and *Plg*-deficient mice. **(A)** Scatter plot of the relative re-epithelialization of wounds day 10 after incision in wild-type mice, *tPA*-deficient mice, *uPA*-deficient mice, *uPA;tPA* double-deficient mice and *Plg*-deficient mice (AI). The relative re-epithelialization was determined as the distance from the wound edge to the front of the leading-edge keratinocytes, divided by the distance between the two wound edges. Examples of keratin-stained sections of day 10 wounds from wild-type mice (AII), *uPA*-deficient mice (AIII), *uPA;tPA* double-deficient mice (AIV) and *Plg*-deficient mice (AV). The red arrows mark the wound edge and black arrows point to the tip of the leading-edge keratinocytes. Bar: II–V ~60  $\mu$ m. **(B)** Scatter plot of the relative re-epithelialization of wounds day 21 after incision in *uPA;tPA* double-deficient mice and *Plg*-deficient mice (BI). Examples of keratin-stained sections of day 21 wounds from *uPA;tPA* double-deficient mice (BII) and *Plg*-deficient mice (BIII). Red arrows mark the wound edge and black arrows identify the tip of the leading-edge keratinocytes. Bar: II–III ~60  $\mu$ m.

healing in both *uPA* single-deficient and *tPA* single-deficient mice is indistinguishable from the healing of wild-type mice. In contrast, the concomitant ablation of both *uPA* and *tPA* caused a significant delay in the healing, in agreement with our previous findings (Bugge *et al*, 1996a). These results clearly demonstrate a functional redundancy between *uPA* and *tPA* in skin wound healing.

The cellular architecture both during and after complete re-epithelialization of the wounds revealed a significant histological difference between *uPA;tPA* double-deficient and *Plg*-deficient mice. The higher residual healing capability of *uPA;tPA* double-deficient mice shows that *Plg* is playing a role in the healing process even in the absence of the two cognate *Plg* activators, *uPA* and *tPA*. *Plg*-deficient mice

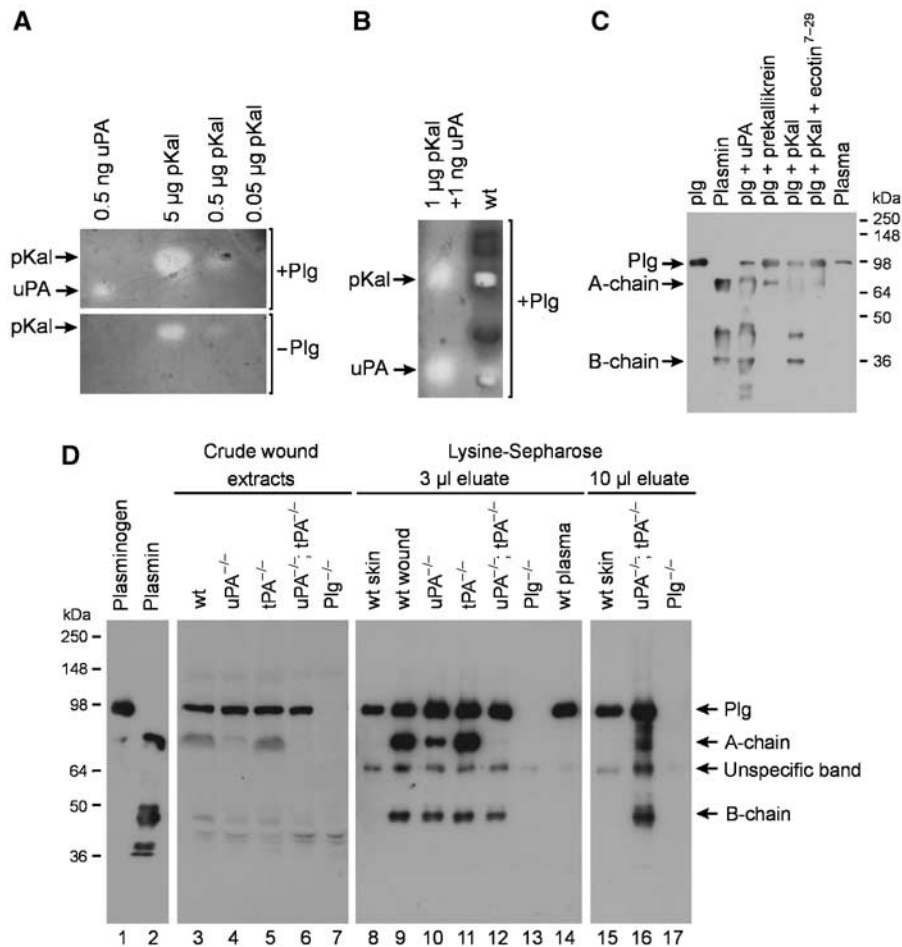


**Figure 5** Detection of fibrinolytic activities and Plg/plasmin in wound extracts. (A) Fibrin/Plg overlay zymography of purified human pKal and murine uPA with and without Plg. Note that the size of the lysis zones generated by pKal decreases in the absence of Plg. (B) Prolonged development of a zymogram with 1 µg of human pKal and 0.1 ng murine uPA in one lane and wild-type 7-day-old incisional wound extract in the second lane reveals activity comigrating with uPA and pKal in the wild-type wound extract. (C) Western blot analysis of 1 µg mouse Plg, 1 µg mouse plasmin and 1 µl of mouse plasma as controls. Generation of plasmin was detected in 1 µg Plg activated for 2 h at 37°C either by 10 ng uPA, 0.1 µg prekallikrein, 0.1 µg pKal or 0.1 µg pKal in the presence of Ecotin<sup>7-29</sup>. (D) Western blot analysis for Plg and plasmin. 1 µg mouse Plg (lane 1), 1 µg mouse plasmin (lane 2). Lanes 3–7: 16 µl of crude wound extract prepared from 7-day-old incisions from either wild-type mice (lane 3), *uPA*-deficient mice (lane 4), *tPA*-deficient mice (lane 5), *uPA*;*tPA* double-deficient mice (lane 6) and *Plg*-deficient mice (lane 7). Lanes 8–14: 3 µl of eluate pool from Lysine-Sepharose columns, wild-type mice skin (lane 8), wild-type mice wounds (lane 9), *uPA*-deficient mice (lane 10), *tPA*-deficient mice (lane 11), *uPA*;*tPA* double-deficient mice (lane 12), *Plg*-deficient mice (lane 13) and plasma from wild-type mice (lane 14). Lanes 15–17: 10 µl of eluate pool from Lysine-Sepharose columns, wild-type mice skin (lane 15), *uPA*;*tPA* double-deficient mice (lane 16) and *Plg*-deficient mice (lane 17).

accumulate abundant fibrin, which disturbs the re-epithelialization process in particular (Rømer *et al*, 1996; Lund *et al*, 1999) and skin wound healing is rescued in double-deficient mice (Bugge *et al*, 1996b). This implies that the impaired healing in *Plg*-deficient mice is caused primarily by impaired fibrinolysis as a consequence of insufficient plasmin generation. Collectively, these data reveal that sufficient levels of plasmin must be generated despite the *uPA*;*tPA* deficiency in these mice, thus implying the presence of an additional Plg activator in these wounds. Accordingly, we have indeed demonstrated the presence of plasmin in wounds from *uPA*;*tPA* double-deficient mice thus providing the first biochemical evidence for an additional plasminogen activator *in vivo*.

A functional overlap exists between Plg and MMPs during skin wound healing (Lund *et al*, 1999) and trophoblast implantation (Solberg *et al*, 2003). We therefore compared the effect of MMP inhibitor treatment on the healing of skin

wounds in *Plg*-deficient mice and *uPA*;*tPA* double-deficient mice. In agreement with our previous study we find that treatment with the MMP inhibitor galardin arrests healing in *Plg*-deficient mice. In *uPA*;*tPA* double-deficient mice, galardin treatment delays the healing process, whereas all the wounds do eventually heal with a mean healing time of 46 days. Two separate conclusions can be drawn from these findings.

Firstly, the further delay of healing in the *uPA*;*tPA* double-deficient mice by blocking MMP activity shows that MMPs contribute to fibrinolysis either directly or indirectly via Plg activation. In further consolidation of this interpretation, we found that galardin treatment of *Plg*;*fibrinogen* double-deficient wounds cause only a moderate delay in healing time (unpublished results) as opposed to the complete block of healing observed in the galardin-treated *Plg*-deficient mice (Lund *et al*, 1999). It remains however to be elucidated which MMP is responsible for fibrin degradation *in vivo*. MMP3, MMP8, MMP9, MMP12, MMP13 and MT1-MMP all have

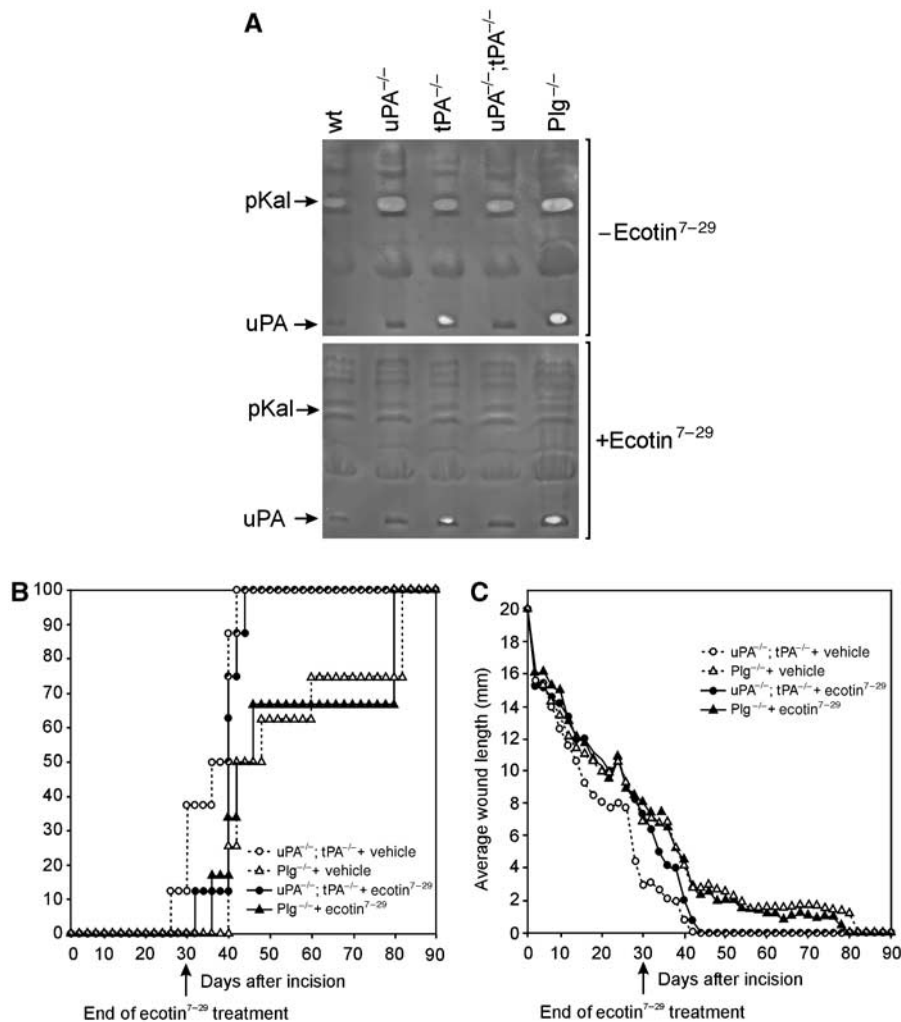


**Figure 6** The pKal inhibitor ecotin<sup>7-29</sup> inhibits plasmin-mediated fibrinolysis and the healing of *uPA;tPA* double-deficient wounds. **(A)** Extracts of 7-day wounds from wild-type, *uPA*-deficient, *tPA*-deficient, *uPA;tPA* double-deficient and *Plg*-deficient mice (pooled from two mice per genotype) were subjected to fibrin/Plg overlay zymography with or without the serine protease inhibitor ecotin<sup>7-29</sup>. Note the complete inhibition of activity corresponding to pKal by ecotin<sup>7-29</sup>, whereas the *uPA* activity is not inhibited. **(B)** *uPA;tPA* double-deficient and *Plg*-deficient mice were treated with the serine protease inhibitor ecotin<sup>7-29</sup> or vehicle for 30 days ( $n = 6-8$ ). The percentage fraction of mice with complete gross healing is plotted versus the time after the incision. **(C)** The wound length plotted versus the time after the incision. Until the end of treatment at day 30 after the incision, the wound length kinetics in ecotin<sup>7-29</sup>-treated *uPA;tPA* double-deficient mice were indistinguishable from vehicle- or ecotin<sup>7-29</sup>-treated *Plg*-deficient mice.

fibrinolytic activities *in vitro* (Bini *et al*, 1996; Hiller *et al*, 2000; Lelongt *et al*, 2001; Hotary *et al*, 2002), but no severe phenotypes after incisional wound healing are reported in the single-deficient mice tested so far; *MMP3*, *MMP9* or *MMP13* (Bullard *et al*, 1999; Mohan *et al*, 2002; Hartenstein *et al*, 2006). This suggests that the fibrinolytic potential of these MMPs should be tested *in vivo* in mice double-deficient in *Plg* and each of these MMPs. Secondly, the pharmacological blocking of MMP-mediated fibrinolysis in *uPA;tPA* double-deficient mice is not sufficient to arrest the healing process, demonstrating that these mice, in contrast to the galardin-treated *Plg*-deficient mice, still possess some residual fibrinolytic potential. This provides evidence of the existence of at least one *Plg* activator in addition to *uPA* and *tPA*, which is not galardin-sensitive.

A previous report suggested that pKal is a *Plg* activator during adipocyte differentiation (Selvarajan *et al*, 2001). We have now confirmed *in vitro* that purified human pKal

has *Plg*-activating activities and, in addition, has some *Plg*-independent fibrinolytic activity. We observed an activity corresponding to pKal in murine wound extracts, and collectively these data suggest that pKal may be involved in fibrin degradation during skin wound healing both directly and through activation of *Plg*. To test this hypothesis, we treated *uPA;tPA* double-deficient mice with a mutated pKal-selective form of the serine protease inhibitor ecotin (Stoop and Craik, 2003), which decreased the healing rate, as measured by the wound length, to a level that was indistinguishable from vehicle-treated *Plg*-deficient wounds. In contrast, treatment of *Plg*-deficient mice with ecotin<sup>7-29</sup> did not lower their healing capacity further. This result suggests that ecotin<sup>7-29</sup> does not inhibit any rate-limiting proteases unrelated to plasminogen activators and the data do not support a biological role of plasminogen independent of its conversion to plasmin in wound healing. Ecotin<sup>7-29</sup> completely blocks the activity of pKal, but not the activity of *uPA* or *tPA* in wound extracts as

determined by fibrin/Plg zymography (Figure 6A and unpublished results). Thus, pKal most likely contributes to skin wound healing through Plg-dependent fibrinolysis.

Prekallikrein, the precursor of pKal is found at high concentrations (40–50 µg/ml) compared to 2–5 ng/ml of pro-uPA in plasma, which may enable its role as a Plg activator *in vivo* despite its relatively poor catalytic efficiency as Plg activator *in vitro* (Colman, 1969). The finding that pKal may play a significant role in Plg activation during skin wound healing suggests that pKal also has important and as yet unidentified physiological functions as a Plg activator in other tissue remodeling processes. Although our results obtained by ecotin<sup>7-29</sup> treatment of *uPA;tPA* double-deficient mice strongly suggest that pKal is an important Plg activator during skin wound healing, we cannot rule out a role for additional Plg activators. Ecotin<sup>7-29</sup> may inhibit other unidentified serine proteases with Plg activator activity, although our overlay zymography strongly support the conclusion that pKal is the additional Plg activator in wound healing. A definitive test of the role of pKal in skin wound healing and other tissue remodelling processes will be possible when *pKal*-deficient mice are available for generation of mice with triple-deficiency for *uPA*, *tPA* and *pKal*. Skin repair in these mice and *Plg*-deficient mice can then be compared directly.

We find it unlikely that the differences between the healing observed in *uPA;tPA* double-deficient and *Plg*-deficient mice can be explained by bacterial infection of the wounds and thereby contamination with prokaryotic Plg activators such as streptokinase or staphylokinase (Sun *et al*, 2004), as no signs of infection have been observed either macroscopically or microscopically in any mice in the experiments. Furthermore, we have observed a similar difference between the phenotypes of *uPA;tPA* double-deficient and *Plg*-deficient mice in a nonlesional tissue remodelling process, that is, post-lactational mammary gland involution, which is less impaired in *uPA;tPA* double-deficient than in *Plg*-deficient mice (unpublished results).

The demonstration of a third Plg activator, which at least partially accounts for the difference in wound healing time between *uPA;tPA*-deficient and *Plg*-deficient mice, has important implications for the understanding of Plg activation during normal and pathological tissue remodelling. It is well established that *Plg* deficiency results in serious physiological consequences in both humans and mice although with different degrees of penetrance (Bugge *et al*, 1995; Schuster *et al*, 1997; Drew *et al*, 1998). In several fundamental physiological processes involving normal as well as pathological tissue remodelling, Plg activation has been shown to play a pivotal role, and it will be interesting to define the individual and combined significance of *uPA*, *tPA* and *pKal*.

Numerous studies have revealed that *uPA* and *uPAR* are expressed either by invading cancer cells or by stromal cells in their vicinity (Johnsen *et al*, 1998). The ability of skin squamous carcinoma cells to mimic the 'invasive' phenotype of re-epithelializing keratinocytes with regard to their expression of components of the Plg activation system and MMPs is likely to reflect a general mechanism employed by invading cancer cells. Our demonstration of the involvement of at least three Plg activators and one or more MMPs in wound healing may thus have important implications for a therapeutic approach aiming at blocking invasion and metastasis in cancer. In order to obtain a complete inhibition of cancer

invasion, it will thus be necessary to use combinations of protease inhibitors.

## Materials and methods

### Animals and animal treatment

*uPA* and *tPA* gene-targeted mice of a mixed 129/Black Swiss background (Carmeliet *et al*, 1994) backcrossed to C57Bl/6J (Panum Institute, Copenhagen) mice for 16 generations were crossed, followed by interbreeding of the double heterozygous offspring. *Plg* gene-targeted 129/Black Swiss mice (Bugge *et al*, 1995) were backcrossed into C57Bl/6J (Panum Institute, Copenhagen) for 21 generations. The plasminogen genotype was determined as described (Lund *et al*, 1999). The *uPA* genotype was determined by multiplex PCR using the following three primers. *muPA*-7p (CTC CCG TGG CTG GGT AGT GG) hybridizing to position 7719–7738 in the mouse *uPA* gene (GenBank: M17922), and *muPA*-4m (AGA GGA CGG TCA GCA TGG GAA C) hybridizing to position 8029–8008 generate a 311 bp product specific for the endogenous allele. *muPA*-4m and *mPGK*-2m (GCC TTG GGA AAA GCG CCT C) hybridizing to position 1092–1074 in the mouse phosphoglycerate kinase-1 promoter (GenBank: X15339) generate a ~186 bp product specific for the targeted allele. The *tPA* genotype was determined by multiplex PCR using the following three primers; *mtPA*-3m (GTC TGT TCT TCC TCT CCG GGG AC) hybridizing to position 1673–1695 in the mouse *tPA* gene (GenBank: AC121835), and *mtPA*-4p (CTC ACA CCC TTG GCA GGC TG) hybridizing to position 1984–1965 generate a 312 bp product specific for the endogenous allele. *mtPA*-3m and *mPGK*-2m generate a ~243 bp product specific for the targeted allele.

All mice used for experiments were males between 6 and 8 weeks old at the start of the experiment. Wound healing experiments of *uPA;tPA*-deficient mice and *Plg*-deficient mice was carried out at the same time and in the same room. Investigators unaware of the mouse genotype performed all experimental evaluations, tissue isolations and microscopic analyses. The MMP inhibitor galardin was synthesized as described (Grobelyny *et al*, 1992). Galardin inhibits the enzymatic activity of a number of MMPs, including MMP2, -3, -9 and -14 (as described in Lund *et al*, 1999). Galardin was formulated as a 20 mg/ml slurry in 4% carboxymethylcellulose (CMC) in PBS and was administered daily i.p. at 100 mg/kg body weight. Mock treatment included 4% CMC in PBS. The same batch of galardin was used for the treatment of *uPA*-, *tPA*- and *Plg*-deficient mice. A mutated form of ecotin rendered highly specific for plasma kallikrein (ecotin<sup>7-29</sup>) was isolated from a phage display library as described (Stoop and Craik, 2003). Samples used for animal injections were diluted in PBS, and administered i.p. at a dose of 10 mg/kg/day (two daily injections for 30 days).

### Tissue preparation

Incisional skin wounds were generated in 6- to 8-week-old mice and tissues were removed for histological analysis as described previously (Lund *et al*, 1999). A total of 133 mice were wounded and tissue isolated at day 10 post-wounding from 18 wild-type mice, 10 *tPA*-deficient, 17 *uPA*-deficient, 13 *uPA;tPA* double-deficient mice and nine *Plg*-deficient mice. At the time of healing, we isolated tissue from 10 wild-type, eight *tPA*-deficient, 11 *uPA*-deficient, six *uPA;tPA* double-deficient mice and five *Plg*-deficient mice. At 1 month post-healing, we isolated tissue from seven wild-type, five *tPA*-deficient, four *uPA*-deficient, five *uPA;tPA* double-deficient mice and five *Plg*-deficient mice. Animal care at The Department of Experimental Medicine, University of Copenhagen and Rigshospitalet, Copenhagen, Denmark was in accordance with the institutional and national guidelines.

### Computer-assisted morphometry

Keratinocyte migration was measured microscopically on tissue sections stained immunohistochemically with anti-keratin IgG (Lund *et al*, 1999). The length of the epidermal tongue was measured as the distance between the tip of the leading-edge keratinocytes and the edge of the wound, defined as the point in the zone of proliferation where a shift from two to three layers of keratinocytes could be identified. The relative migration was determined as the sum of the lengths of both epidermal tongues divided by the width of the wound, defined as the distance between

the wound edges. Indication of this point in the proliferation zone and the tip of the epidermal wedge by image analysis (Olympus AX70 system) were performed by an observer unaware of the genotype of the mice. The mean fraction of migration, the standard error (s.e.) was determined for each group of animals.

### Statistical analysis

The SAS<sup>®</sup> software package (version 8.2; SAS Institute, Cary, NC) was used to manage data and for statistical analysis. The distribution of time to wound closure was found to be normal. Prespecified tests of hypothesis comparing experimental groups to the control group of mice were carried out using two sample *t*-tests. The assumption of variance homogeneity was tested by the folded *F*-test and the two sample *t*-test assuming unequal variances was used if the hypothesis of variance homogeneity was rejected. Incomplete data were discarded. Power calculations demonstrated that at least eight mice should be included in each group in order to detect a difference in time to wound closure of 5 days with 80% power. Plots of time to complete re-epithelialization were carried out using Kaplan–Meier estimates. The level of significance was set at 5%.

### Zymography

Wound tissue containing both the wound rim and granulation tissue was lysed in 5  $\mu$ l of 0.1 M Tris/HCl, 1% Triton X-100, pH 7.4 per mg wet weight of tissue. The extracts were used for fibrin/Plg overlay zymograms with and without plasminogen as described (Lund *et al*, 1996) and with and without ecotin<sup>7–29</sup> (10  $\mu$ g/ml) followed by incubation at 37°C for 16–28 h or in prolonged development for 40 h. Recombinant mouse pro-uPA (produced by Schneider cells, as described previously (Ploug *et al*, 2001)) and human plasma kallikrein (Kordia Life Sciences, The Netherlands) were used as controls.

### Western blot analysis

Frozen tissue powder containing both the wound rim and granulation tissue (pool of three mice per genotype) was resuspended in 5  $\mu$ l of 0.1 M Tris/HCl, pH 7.4, 10  $\mu$ g/ml of aprotinin per mg wet weight of tissue, treated for 2  $\times$  8 min on an Ultrasound bath and the resulting supernatants were collected after centrifugation at 12000g for 30 min at 4°C. Samples were reduced and alkylated before SDS–PAGE and transferred to PVDF membranes by electroblotting. Additional binding was blocked by incubation for 1 h at room temperature with 5% nonfat-dried milk in phosphate-buffered saline containing 0.05% Tween-20 (PBS-T). Incubation with the primary antibody was overnight at 4°C with 0.5  $\mu$ g/ml polyclonal rabbit anti-human plasminogen antibody (DAKO, A0081). After washing in PBS-T (5  $\times$  5 min), membranes were incubated for 1½ h at room temperature with HRP-linked secondary antibody (DAKO, P0217) diluted 1:5000 in blocking buffer. After washing in PBS-T and PBS, HRP activity was detected using

enhanced chemiluminescence's reagents (Amersham Biosciences, Hillerød, Denmark). Purified mouse Plg and plasmin (Innovative Research, Inc., Hilltop, MI) were used as controls. A negative control without primary antibody included was carried out in parallel.

One-step affinity purification of Plg/plasmin was accomplished by application of 1500  $\mu$ l wound extract onto 100  $\mu$ l lysine Sepharose 4B gel (Amersham Bioscience) settled in a disposable column. After sample application, the columns were washed extensively with more than 10 column volumes of 0.1 M phosphate buffer, pH 7.4. The bound Plg/plasmin were eluted by 250  $\mu$ l 0.1 M 6-aminohexanoic acid in 0.1 M phosphate buffer, pH 7.4 and fractions of approximately 25  $\mu$ l were collected. All manipulations were performed at 4°C with buffers containing 10  $\mu$ g/ml aprotinin.

### Double immunofluorescence

Tissue sections were deparaffinized in xylene and hydrated through graded ethanol/water dilutions. Antigen retrieval was carried out by incubation with proteinase K for 15 min at 37°C. Sections were washed in running tap water for 5 min and Tris-buffered saline (TBS: 50 mM Tris, 150 mM NaCl, pH 7.6) for 5 min. Sections were incubated overnight simultaneously with both rabbit anti-mouse fibrin(ogen) antibody (1:2000; Bugge *et al*, 1995) and rat anti-mouse Tromal antibody (detects cytokeratin 8; 1:100 Kemler *et al*, 1981), in TBS containing 0.25% BSA at 4°C. Rabbit anti-fibrin(ogen) antibody was detected with Alexa Fluor 488-linked donkey anti-rabbit antibody (1:200, Molecular Probes, CA, A21206) and rat anti-Troma-1 antibody was detected with Alexa Fluor 594-linked goat anti-rat antibody (1:200, Molecular Probes, A11007) diluted together in TBS containing 0.25% BSA and incubated for 45 min at room temperature. Antibody incubations were followed by washes in TBS. Controls without anti-fibrin(ogen) primary antibody were negative for unspecific staining.

### Acknowledgements

We thank Dr Thomas Bugge for the *Plg*-deficient mice and Dr Peter Carmeliet for the *uPA*- and *tPA*-deficient mice. We are grateful to Mette M Andersen, Lotte Frederiksen, Kirsten L Jakobsen, Charlotte Lønberg and John Post for excellent technical assistance. This work was supported financially by the European Commission: Grant number QLGI-CT-2000-01131 and LSHC-CT-2003-503297, European Union research training grant for mammary gland biology RTN-2002-00246, Aage Bangs Foundation, the Danish Biotechnology Program, Centre for Medical Biotechnology, the Danish Cancer Society, the Danish Medical Research Council, the Danish Cancer Research Foundation, Agnes and Poul Friis Foundation and a grant from the National Cancer Institute (USA) P01 CA072006.

### References

- Beare AHM, O'Kane S, Krane SM, Ferguson MWJ (2003) Severely impaired wound healing in the collagenase-resistant mouse. *J Invest Dermatol* **120**: 153–163
- Bini A, Itoh Y, Kudryk BJ, Nagase H (1996) Degradation of cross-linked fibrin by matrix metalloproteinase 3 (stromelysin 1): hydrolysis of the gamma Gly 404-Ala 405 peptide bond. *Biochemistry* **35**: 13056–13063
- Bugge TH, Flick MJ, Danton MJ, Daugherty CC, Rømer J, Danø K, Carmeliet P, Collen D, Degen JL (1996a) Urokinase-type plasminogen activator is effective in fibrin clearance in the absence of its receptor or tissue-type plasminogen activator. *Proc Natl Acad Sci USA* **93**: 5899–5904
- Bugge TH, Flick MJ, Daugherty CC, Degen JL (1995) Plasminogen deficiency causes severe thrombosis but is compatible with development and reproduction. *Genes Dev* **9**: 794–807
- Bugge TH, Kombrinck KW, Flick MJ, Daugherty CC, Danton MJ, Degen JL (1996b) Loss of fibrinogen rescues mice from the pleiotropic effects of plasminogen deficiency. *Cell* **87**: 709–719
- Bugge TH, Lund LR, Kombrinck KK, Nielsen BS, Holmback K, Drew AF, Flick MJ, Witte DP, Danø K, Degen JL (1998) Reduced metastasis of Polyoma virus middle T antigen-induced mammary cancer in plasminogen-deficient mice. *Oncogene* **16**: 3097–3104
- Bullard KM, Lund L, Mudgett JS, Mellin TN, Murphy B, Ronan J, Banda MJ (1999) Impaired wound contraction in stromelysin-1 deficient mice. *Ann Surg* **230**: 260–265
- Carmeliet P, Schoonjans L, Kieckens L, Ream B, Degen J, Bronson R, De Vos R, van den Oord JJ, Collen D, Mulligan RC (1994) Physiological consequences of loss of plasminogen activator gene function in mice. *Nature* **368**: 419–424
- Collen D, Lijnen HR (2005) Thrombolytic agents. *Thromb Haemost* **93**: 627–630
- Colman RW (1969) Activation of plasminogen by human plasma kallikrein. *Biochem Biophys Res Commun* **35**: 273–279
- Danø K, Andreasen PA, Grøndahl-Hansen J, Kristensen P, Nielsen LS, Skriver L (1985) Plasminogen activators, tissue degradation, and cancer. *Adv Cancer Res* **44**: 139–266
- Danø K, Behrendt N, Hoyer-Hansen G, Johnsen M, Lund LR, Ploug M, Romer J (2005) Plasminogen activation and cancer. *Thromb Haemost* **93**: 676–681

- Danø K, Romer J, Nielsen BS, Bjorn S, Pyke C, Rygaard J, Lund LR (1999) Cancer invasion and tissue remodeling—cooperation of protease systems and cell types. *Apmis* **107**: 120–127
- Drew AF, Kaufman AH, Kombrinck KW, Danton MJ, Daugherty CC, Degen JL, Bugge TH (1998) Ligneous conjunctivitis in plasminogen-deficient mice. *Blood* **91**: 1616–1624
- Egeblad M, Werb Z (2002) New functions for the matrix metalloproteinases in cancer progression. *Nat Rev Cancer* **2**: 161–174
- Ellis V, Behrendt N, Dano K (1991) Plasminogen activation by receptor-bound urokinase. A kinetic study with both cell-associated and isolated receptor. *J Biol Chem* **266**: 12752–12758
- Grobelny D, Ponez L, Galardy RE (1992) Inhibition of human skin fibroblast collagenase, thermolysin and *Pseudomonas aeruginosa* elastase by peptide hydroxamic acids. *Biochemistry* **31**: 7152–7154
- Hartenstein B, Dittrich BT, Stickens D, Heyer B, Vu TH, Teurich S, Schorpp-Kistner M, Werb Z, Angel P (2006) Epidermal development and wound healing in matrix metalloproteinase 13-deficient mice. *J Invest Dermatol* **126**: 486–496
- Hiller O, Lichte A, Oberpichler A, Kocourek A, Tschesche H (2000) Matrix metalloproteinases collagenase-2, macrophage elastase, collagenase-3, and membrane type 1-matrix metalloproteinase impair clotting by degradation of fibrinogen and factor XII. *J Biol Chem* **275**: 33008–33013
- Hotary KB, Yana I, Sabeh F, Li XY, Holmbeck K, Birkedal-Hansen H, Allen ED, Hiraoka N, Weiss SJ (2002) Matrix metalloproteinases (MMPs) regulate fibrin-invasive activity via MT1-MMP-dependent and -independent processes. *J Exp Med* **195**: 295–308
- Johnsen M, Lund LR, Rømer J, Almholt K, Danø K (1998) Cancer invasion and tissue remodeling: common themes in proteolytic matrix degradation. *Curr Opin Cell Biol* **10**: 667–671
- Kemler R, Brulet P, Schnebelen M T, Gaillard J, Jacob F (1981) Reactivity of monoclonal antibodies against intermediate filament proteins during embryonic development. *J Embryol Exp Morphol* **64**: 45–60
- Lelongt B, Bengatta S, Delauche M, Lund LR, Werb Z, Ronco PM (2001) Matrix metalloproteinase 9 protects mice from anti-glomerular basement membrane nephritis through its fibrinolytic activity. *J Exp Med* **193**: 793–802
- Llinas P, Le Du MH, Gardsvoll H, Dano K, Ploug M, Gilquin B, Stura EA, Menez A (2005) Crystal structure of the human urokinase plasminogen activator receptor bound to an antagonist peptide. *EMBO J* **24**: 1655–1663
- Lund LR, Bjørn SF, Sternlicht MD, Nielsen BS, Solberg H, Usher PA, Osterby R, Christensen IJ, Stephens RW, Bugge TH, Dano K, Werb Z (2000) Lactational competence and involution of the mouse mammary gland require plasminogen. *Development* **127**: 4481–4492
- Lund LR, Rømer J, Bugge TH, Nielsen BS, Frandsen TL, Degen JL, Stephens RW, Danø K (1999) Functional overlap between two classes of matrix-degrading proteases in wound healing. *EMBO J* **18**: 4645–4656
- Lund LR, Rømer J, Thomasset N, Solberg H, Pyke C, Bissell MJ, Danø K, Werb Z (1996) Two distinct phases of apoptosis in mammary gland involution: proteinase-independent and -dependent pathways. *Development* **122**: 181–193
- Madlener M, Parks WC, Werner S (1998) Matrix metalloproteinases (MMPs) and their physiological inhibitors (TIMPs) are differentially expressed during excisional skin wound repair. *Exp Cell Res* **242**: 201–210
- Mohan R, Chintala SK, Jung JC, Villar WV, McCabe F, Russo LA, Lee Y, McCarthy BE, Wollenberg KR, Jester JV, Wang M, Welgus HG, Shipley JM, Senior RM, Fini ME (2002) Matrix metalloproteinase gelatinase B (MMP-9) coordinates and effects epithelial regeneration. *J Biol Chem* **277**: 2065–2072
- Ploug M (2003) Structure–function relationships in the interaction between the urokinase-type plasminogen activator and its receptor. *Curr Pharm Des* **9**: 1499–1528
- Ploug M, Ostergaard S, Gardsvoll H, Kovalski K, Holst-Hansen C, Holm A, Ossowski L, Danø K (2001) Peptide-derived antagonists of the urokinase receptor. Affinity maturation by combinatorial chemistry, identification of functional epitopes, and inhibitory effect on cancer cell intravasation. *Biochemistry* **40**: 12157–12168
- Rømer J (2003) Skin cancer and wound healing: tissue-specific similarities in extracellular proteolysis. *APMIS* **111** (Suppl 107): 1–36
- Rømer J, Bugge TH, Pyke C, Lund LR, Flick MJ, Degen JL, Dano K (1996) Impaired wound healing in mice with a disrupted plasminogen gene. *Nat Med* **2**: 287–292
- Schuster V, Mingers AM, Seidenspinner S, Nussgens Z, Pukrop T, Kreth HW (1997) Homozygous mutations in the plasminogen gene of two unrelated girls with ligneous conjunctivitis. *Blood* **90**: 958–966
- Selvarajan S, Lund LR, Takeuchi T, Craik CS, Werb Z (2001) A plasma kallikrein-dependent plasminogen cascade required for adipocyte differentiation. *Nat Cell Biol* **3**: 267–275
- Solberg H, Rinkenberger J, Danø K, Werb Z, Lund LR (2003) A functional overlap of plasminogen and MMPs regulates vascularization during placental development. *Development* **130**: 4439–4450
- Stoop AA, Craik CS (2003) Engineering of a macromolecular scaffold to develop specific protease inhibitors. *Nat Biotechnol* **21**: 1063–1068
- Sun H, Ringdahl U, Homeister JW, Fay WP, Engleberg NC, Yang AY, Rozek LS, Wang X, Sjobring U, Ginsburg D (2004) Plasminogen is a critical host pathogenicity factor for group A streptococcal infection. *Science* **305**: 1283–1286